

Lifetime of a two-dimensional air bubble

Ayako Eri and Ko Okumura*

Department of Physics, Graduate School of Humanities and Sciences, Ochanomizu University, 2-1-1, Otsuka, Bunkyo-ku, Tokyo 112-8610, Japan

(Received 16 March 2007; revised manuscript received 24 October 2007; published 6 December 2007)

Air bubbles created in many viscous liquids rise up to the liquid-air interface and stay there for a while before exploding and disappearing. The lifetimes of such bubbles are governed by the thinning dynamics of the hemispherical liquid film separating the bubble from bulk air. Here, the lifetime of bubbles confined by two separated wetting plates is experimentally studied as the distance apart, viscosity, and bubble size are changed. Although the film is not hemispherical but takes a nontrivial shape, a relatively simple hydrodynamic model accounts for the observations.

DOI: [10.1103/PhysRevE.76.060601](https://doi.org/10.1103/PhysRevE.76.060601)

PACS number(s): 68.15.+e, 47.15.gp, 47.55.dd

A child often gets into mischief making bubbles with a straw in milk. Likewise, in daily life, in many industrial situations (e.g., polymer foam) [1], and even in volcanic eruptions, air bubbles can remain at the liquid-air interface before exploding and disappearing, whether with or without surfactant (soap film [2] or “bare” film [3]). The lifetimes of such bubbles are controlled by the thinning dynamics of the hemispherical liquid film separating the bubble from bulk air. It is known that the dynamics is dictated by the liquid boundary conditions at the interface [3,4]. However, the lifetime of bubbles confined in two-dimensional space by two plates separated by a distance D has not been studied; in this confined case the film is not hemispherical but takes a nontrivial shape. Here we show that the thinning dynamics of a bare film sandwiched by two wetting plates (Fig. 1) can be described by surprisingly simple boundary conditions. We experimentally obtained the lifetimes of the two-dimensional bubbles when the liquid viscosity, distance D , and bubble size were changed and find that the dependence of the lifetime on these variables can be well understood by a simple hydrodynamic model completed with nontrivially simplified boundary conditions. We anticipate that our demonstration will lead to studies on a rich variety of film thinning dynamics of bubbles occurring in different practical situations; for example, the situation when the two plates repel the liquid film, as opposed to the present study, or when a liquid bubble is created in another liquid, will be relevant for such developments. In addition, our work will ignite a series of studies of novel bursting dynamics of film encapsulating two-dimensional bubbles in various situations.

We use a Hele-Shaw cell of centimeter dimensions made from two transparent acrylic boards of millimeter thickness. The boards are separated by a distance D , with acrylic spacers of homogeneous thickness. We fill the cell with a polydimethylsiloxane melt and inject a bubble from the bottom of the cell. The bubble slowly rises in the melt until it settles at the liquid-air interface, forming a semicircular shape of radius R .

This quasistatic form could survive for a few minutes at

the surface of a viscous liquid in the Hele-Shaw cell until the bubble suddenly burst and disappeared. We study the change of the thickness h in time of the liquid film of such a bubble by taking magnified snapshots with a video camera (HC-1, Sony) with a macro lens (MSN-505, Raynox) as shown in Fig. 1(b) (the quasistatic shape and the dynamics of bursting will be reported elsewhere). The combination of the liquid and the cell material establishes complete wetting with zero contact angle.

The result of the measurement of h as a function of time t is summarized in Fig. 2. As stipulated in Table I, we change the liquid kinematic viscosity ν from 500 to 1000 centistokes (cS) (500 to 1000 times the viscosity of water) and the cell separation D from 0.5 to 1.0 mm for centimeter-size bubbles (precise experimental control of R is difficult), to infer a universal relation applicable to a wide range of scales. From the figure, we can conclude that the thinning dynamics depends nontrivially on the three parameters ν , D , and R . This dependence will be clarified below both from a simple theory and from a detailed analysis of these data based on the theory.

Here, let us recall some of the basic theoretical considerations pertinent to the present phenomenon. The drainage from a flat circular disk of fluid film subject to a constant force sandwiching the disk is discussed, for example, in [6]. The dynamics are distinguished by the boundary conditions at the liquid-air interface: (a) in the Poiseuille-flow regime the velocities at the two liquid surfaces are zero, producing a

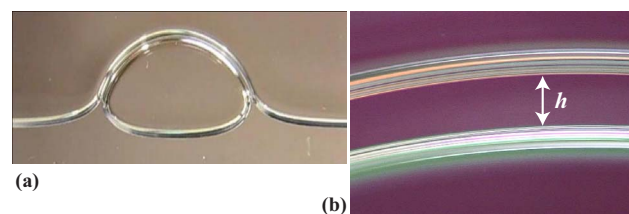


FIG. 1. (Color online) (a) Two-dimensional air bubble sitting at the liquid-air interface of a Hele-Shaw cell. This quasistatic shape could be maintained for a few minutes. (b) Magnified view of the upper wall of the bubble in (a). The film of a well-defined thickness h possesses sharp edges at the top and bottom, followed by fringes. A short movie is available [5].

*Author to whom correspondence should be addressed; okumura@phys.ocha.ac.jp

TABLE I. Experimental parameters corresponding to the labeling in Fig. 2, together with the experimentally obtained τ and h_0 (see below).

	A1	A2	B1	B2	C1	C2
ν (cS)	500	500	1000	1000	500	500
D (mm)	0.5	0.5	1	1	1	1
R (mm)	21.1	20.9	21.3	13.1	13.0	10.7
τ (s)	52.9	44.4	22.4	15.6	8.20	7.45
h_0 (mm)	0.694	0.768	0.537	0.509	0.300	0.254

velocity gradient in the direction of the film thickness, and (b) in the plug-flow regime the velocity is homogeneous in the direction of the film thickness, suggesting a slip of the film at the boundary. The former results in a nonexponential law in time for the drainage and the latter in an exponential law in time.

These considerations are extended to the case of a liquid film of a three-dimensional bubble sitting at the surface of a viscous liquid filling a beaker [3]. In such a case, drainage from a hemispherical shell of liquid film occurs because of gravity when the bubble radius R is larger than the capillary length, implying that the gravity excels the capillary force as the driving force, where the gravitational drive is hindered by viscous friction. In this case of a free-standing bare film (without surfactants), the plug-flow condition is found to be appropriate, which leads to an exponential law $h \cong h_0 \exp(-t/\tau)$ with $1/\tau \cong gR/\nu$ (g is the gravitational constant). This law is confirmed by experiment in [3].

Recently, the nonexponential law in the opposite regime of Poiseuille flow was experimentally confirmed [4] in a slightly different context, where a hemispherical thin air film is surprisingly formed between bulks of the same liquid. When a drop of radius larger than the capillary length is deposited on a vibrating bath of the same liquid, the drop can remain at the interface for a while even after the vibration is stopped, which can be seen as one variation of the ‘‘anti-bubble’’ [7]. Thinning of the air film can be measured regardless of the bath vibration, which leads to the predicted non-exponential power law for the Poiseuille flow.

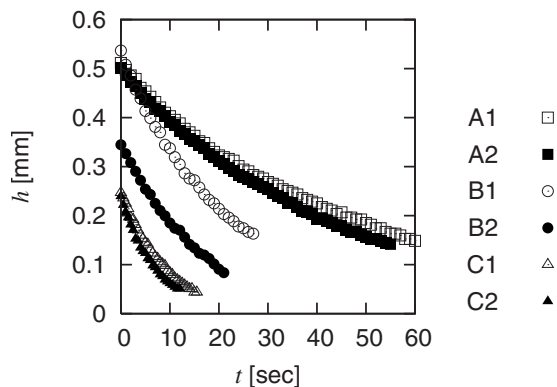


FIG. 2. Change of the film thickness h (mm) with time t (s). Experimental parameters ν , D , and R for the labels employed in this figure are summarized in Table I.

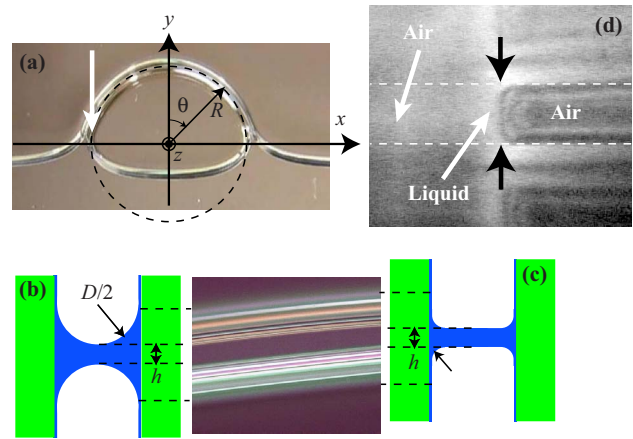


FIG. 3. (Color online) (a) Definition of the (r, θ, z) coordinates for a bubble. The z axis is perpendicular to this paper. (b) Possible side view (section) of the film. (c) Actual side view. One of the rounded corners is indicated by the arrow. (d) Direct view, from the direction and of the point, which direction and point are indicated by the white arrow in (a). Two white dashed lines correspond to the surfaces of the acrylic boards. Two black arrows indicate the liquid-air interface (the other interface on the left is out of focus).

In the present two-dimensional case, the situation is rather different as shown in Fig. 3, where the (r, θ, z) coordinates are defined. The first difference is that the film is not like a hemispherical shell. One would think that the film is sandwiched by top and bottom interfaces of curvatures $1/(R+h/2)-2/D$ and $1/(R-h/2)+2/D$ [Fig. 3(b)] where R ($\gg h$) is the local curvature of the film in the plane parallel to the cell plates [Fig. 3(a)]: since the liquid totally wets the cell plates with zero contact angle, the contour of the section of the liquid film would be comprised of two semicircles of radius $D/2$. This complex shape would lead to formidable boundary conditions. However, the fringes at the top and bottom of the sharp film edges indicate a film of thickness h abruptly merging to a thin liquid layer of micrometer thickness with zero contact angle [Fig. 3(c)], which is confirmed in Fig. 3(d). The non-trivial shape in Fig. 3(c), established by the direct observation and similar to the shapes observed frequently in liquid foams, is dynamically stable, as opposed to the shape in 3(b), although the latter is favorable in terms of surface energy; in Fig. 3(c), the pressure inside the micrometer film along the acrylic boards and the pressure inside the film of thickness h are almost the same as the atmospheric pressure and these pressures are higher than the pressure around the rounded corner indicated by the slant arrow in Fig. 3(c); liquid tends to be attracted to the corner but the movement is prohibited because there is no sink for the attracted liquid.

The second difference is that in the present case the velocity distribution of the flow is more complicated. However, the dynamics inside the curved slab portion of thickness h [see Fig. 4(c)] is not too complex where the dominant component v of the velocity is the θ component, although the flow near the rounded corners [see Fig. 3(c)] is intricate. Inside the slab, the prominent velocity component v is a Poiseuille flow in the z direction because $v(z=\pm D/2)=0$

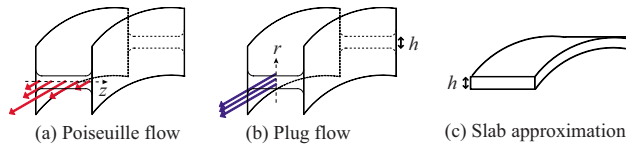


FIG. 4. (Color online) A portion of the liquid film in question (oblique perspective view) with two possible modes of velocity distribution of the flow inside it: (a) Poiseuille flow in the z direction and (b) Plug flow in the r direction. (c) Slab approximation of this portion.

[Fig. 4(a)] while it is like a plug flow in the r direction because $\partial v / \partial n = 0$ at the upper and lower liquid-air surfaces, where n denotes the normal direction [Fig. 4(b)].

This suggests that the velocity inside the slab changes predominantly in the z direction with a length scale D in the lubricant equation

$$\nu \nabla^2 v(\theta, z) = -g \sin \theta, \quad (1)$$

which gives a velocity $V \approx (gD^2/\nu)\sin \theta$ averaged over the z direction. Note here that the numerical coefficient of this relation is exactly $1/12$ within the slab approximation, which neglects the effect of the rounded corners.

The flow flux inside the slab $Q = D \int_{R-h/2}^{R+h/2} dr V \approx (gD^3 h/\nu)\sin \theta$ is practically preserved, i.e.,

$$D \frac{\partial h}{\partial t} = -\frac{\partial Q}{R \partial \theta}, \quad (2)$$

which leads to an exponential law

$$h = h_0 \frac{\exp(-t/\tau)}{\cos^2(\theta/2)} \quad (3)$$

with the relaxation time τ , or a measure of the lifetime of a bubble, specified by

$$\frac{1}{\tau} = \frac{gD^2}{12R\nu}, \quad (4)$$

where we have used the numerical factor $1/12$ for V throughout the inside of the slab. This approximation is good as long as h is not too thin for the corner effect to be non-negligible.

Here we give some remarks on the comparison with the three-dimensional theories. (1) If the essential direction over which the velocity changes is the θ direction, whose length scale is R , we recover the relaxation time $1/\tau \approx gR/\nu$ of the three-dimensional plug-flow dynamics. (2) In the three-dimensional case, the Poiseuille flow results in a nonexponential law, while here this is not the case, and we obtain an exponential law in the two-dimensional case due to the extra length scale D .

To examine the validity of the above arguments, we first obtain a measure of the lifetime τ (and h_0) from data in Fig. 2 by fitting them with Eq. (3) with $\theta=0$ [in all the measurements, the approximation $\cos^2(\theta/2)=1$ is almost precise], as in Table I. When all the data in Fig. 2 are renormalized by h_0 and τ thus obtained we get Fig. 5: Eq. (3) works quite well. Note that the data shown in Fig. 2 are only the ones corre-

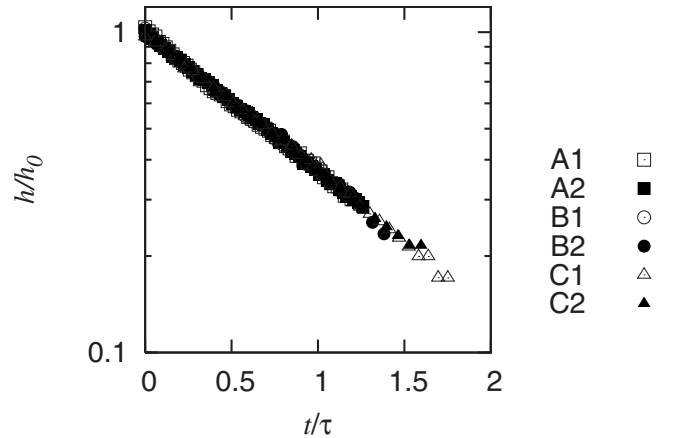


FIG. 5. Result of fitting of the data points in Fig. 2 by Eq. (3) with $\theta=0$ to confirm the exponential law and to extract experimental values of τ (and h_0) for different ν , D , and R .

sponding to long-time regions where the lubrication approximation invoked above is expected to work well; the approximation neglects the inertial term in the Navier-Stokes equation, which is justified at long times when the relation $t > \tau_0$ holds, where τ_0 is determined by balancing the inertial term with the viscous term, i.e., $\tau_0 \approx D^2/\nu$, so that $\tau_0 \approx 0.001$ s for $\nu=1000$ cS and 0.01 s for $\nu=500$ cS, while we start the measurements summarized in Fig. 2 a little after the thinning dynamics sets in.

Now that the validity of Eq. (3) is confirmed, we check Eq. (4). For this purpose, we first determine the local curvature R directly from the snapshots. Using the values of R thus obtained and of τ determined by the process of fitting to produce Fig. 5, we then plotted the relations between $1/\tau$ and ν , those between $1/\tau$ and D , and those between $1/\tau$ and R , in Figs. 6(a)–6(c), respectively, with the theoretical curve based on Eq. (4) drawn as a dotted curve in each figure.

We see that the relation in Eq. (4) agrees well with the behavior of the relaxation time τ obtained by experiments. This agreement without any fitting parameters suggests that the corner effects are actually negligible in a wide range of h , so that the lifetime formula in Eq. (4) with the coefficient $1/12$ is useful in practice.

What if the plug-flow condition in the r direction is replaced by the Poiseuille condition? Experimentally, such a situation could be realized, for example, by filling the cell with glycerin and then with viscous oil (where the glycerin phase is covered from above with the oil phase) and then by injecting a glycerin drop from above. In this case, the velocity changes over the z and r directions with the length scales D and h , respectively, so that ∇^2 in Eq. (1) scales as $1/h^2$ when $h < D$, which renders the thinning dynamics nonexponential and independent of D :

$$h = R \left(\frac{\tau}{t + t_0} \right)^{1/2} \quad (5)$$

with $1/\tau \approx \rho g R / \eta$. Here, ρ is the density difference between the two liquids and η is the viscosity of the liquid forming the film. The law in Eq. (5) is essentially the same as that

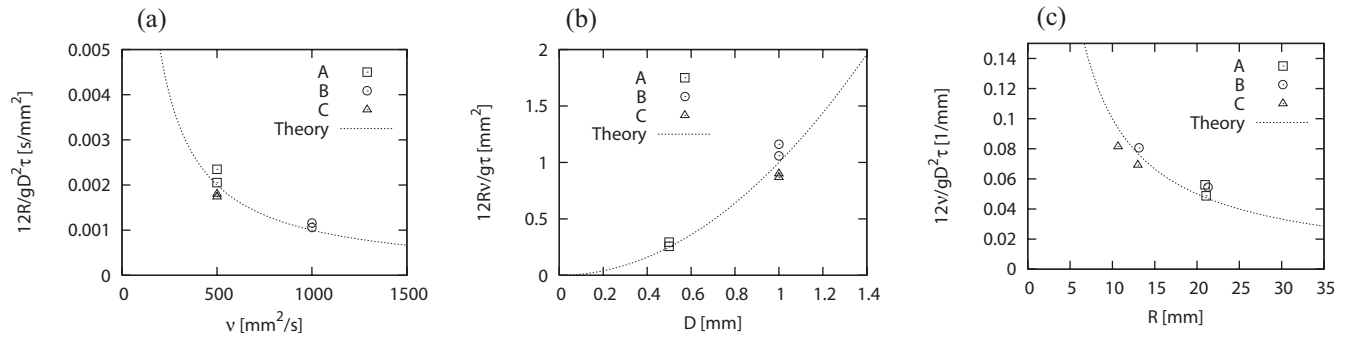


FIG. 6. Relations between $1/\tau$ and (a) ν , (b) D , and (c) R . In all the plots, we use R measured from snapshots and τ obtained by experiments. The dotted curve in each plot corresponds to Eq. (4), which is drawn without any fitting parameters. The labelings A, B, and C correspond to (A1, A2), (B1, B2), and (C1, C2) in Fig. 2 and Table I.

confirmed for the thinning dynamics of an air film created between bulks of the same liquid in [4], although the situation seems to be rather different at first sight. Realization of the experiments suggested here is now under study, together with another series of experiments of adding surfactants to the liquid, which is another possibility to change the boundary conditions.

To understand the full physics of the lifetime of the film, we need to study the bursting of the fluid film [3,4,8], closely related to many important aspects of wetting such as dewetting of a polymer film on the substrate [9], in addition to the associated instability and nucleation which initiates the bursting, although they are smaller in time scales, and thus the thinning dynamics studied here is most important to understand the lifetime. However, since the thinning dynamics has turned out to be markedly different depending on the dimensionality, the study of the bursting, instability, and nucleation of the present two-dimensional film is worthwhile, which is also now under way.

In conclusion, we examine the thinning dynamics of a liquid film of a two-dimensional bubble sandwiched by two plates when the liquid totally wets the plates. We experimentally confirmed that the exponentially decaying dynamics is governed by the gravitational drive opposed by a viscous friction from the Poiseuille flow between the two plates: the theoretical predictions given in Eqs. (3) and (4) are well confirmed by experiment (at $\theta \ll 1$). Our demonstration will be developed to studies on a rich variety of thinning dynamics and bursting of liquid film encapsulating two-dimensional bubbles.

The authors are grateful to an anonymous referee for deep comments which advanced our understanding of this phenomenon significantly. They also thank Akane Suzuki and Reina Kato (Ochanomizu University) for Fig. 1(a) and K. Yaegashi-Nakaya and M. Imai (O.U.) for partial confirmation of the liquid viscosity. K.O. thanks MEXT, Japan for KAKENHI.

-
- [1] D. Weaire and S. Hutzler, *The Physics of Foams* (Clarendon Press, Oxford, 1999).
 [2] K. Mysels, K. Shinoda, and S. Frenkel, *Soap Films* (Pergamon, London, 1959).
 [3] G. Debrégeas, P.-G. de Gennes, and F. Brochard-Wyart, *Science* **279**, 1704 (1998).
 [4] Y. Couder, E. Fort, C.-H. Gautier, and A. Boudaoud, *Phys. Rev. Lett.* **94**, 177801 (2005).
 [5] See EPAPS Document No. E-PLLEE8-76-R13711 for the

- movie of this experiment. For more information on EPAPS, see <http://www.aip.org/pubservs/epaps.html>.
 [6] G. Debrégeas, Thèse, Université Paris IV, 1997.
 [7] S. Dorbolo, E. Reyssat, N. Vandewalle, and D. Quere, *Europhys. Lett.* **69**, 966 (2005).
 [8] E. Reyssat and D. Quéré, *Europhys. Lett.* **76**, 236 (2006).
 [9] G. Reiter, M. Hamieh, P. Damman, S. Slavovs, S. Gabriele, T. Vilmin, and E. Raphaël, *Nat. Mater.* **4**, 754 (2005).